A Test of the Adhesion Approximation for Gravitational Clustering

Adrian L. Melott,[1] Sergei F. Shandarin,[1] and David H. Weinberg[2]

[1] Department of Physics and Astronomy
University of Kansas
Lawrence, Kansas 66045, USA
[2]Institute for Advanced Study
Princeton, New Jersey 08540, USA

A Test of the Adhesion Approximation for Gravitational Clustering

Adrian L. Melott,[1] **Sergei F. Shandarin,**[1] and **David H. Weinberg**[2]

[1] Department of Physics and Astronomy, University of Kansas, Lawrence, Kansas 66045
[2] Institute for Advanced Study, Princeton, New Jersey 08540

ABSTRACT

We quantitatively compare a particle implementation of the adhesion approximation to fully non–linear, numerical "N–body" simulations. Our primary tool, cross–correlation of N–body simulations with the adhesion approximation, indicates good agreement, better than that found by the same test performed with the Zel'dovich approximation (hereafter ZA). However, the cross–correlation is not as good as that of the truncated Zel'dovich approximation (TZA), obtained by applying the Zel'dovich approximation after smoothing the initial density field with a Gaussian filter. We confirm that the adhesion approximation produces an excessively filamentary distribution. Relative to the N–body results, we also find that: (a) the power spectrum obtained from the adhesion approximation is more accurate than that from ZA or TZA, (b) the error in the phase angle of Fourier components is worse than that from TZA, and (c) the mass distribution function is more accurate than that from ZA or TZA. It appears that adhesion performs well statistically, but that TZA is more accurate dynamically, in the sense of moving mass to the right place.

Subject Heading: Galaxies, formation, clustering–large–scale structure of the Universe

I. INTRODUCTION

The large–scale structure of the Universe is thought to have arisen from primarily gravitational processes acting to amplify primordial density fluctuations. In the limit of small fluctuations, the differential equations for the density contrast can be solved by linear perturbation theory (see, e.g., Peebles [1980]). Zel'dovich (1970) proposed an approximation in which the linear–order particle velocities are extrapolated, instead of the linear density contrast. It has often been supposed that this approximation is appropriate only for initial fluctuation spectra with very little power on small scales. However, Coles, Melott and Shandarin (1993; hereafter CMS) compared a number of approximate schemes for gravitational evolution, starting from initial conditions with power spectra $P(k) \propto k^n$, and found that the Zel'dovich approximation (hereafter ZA) was the most successful of these for all indices $n \leq +1$.

There is considerable benefit to applying the same tests to a series of approximations, so that they can be compared with each other. In this paper we report the results of applying the CMS tests to the adhesion approximation, proposed by Gurbatov, Saichev and Shandarin (1985, 1989) and implemented in a particle code by Weinberg and Gunn (1990). (For further discussion of the adhesion approximation, see Kofman *et al.* [1992] and references therein).

CMS proposed a simple extension of ZA, obtained by smoothing the initial density field *before* applying ZA, in order to suppress the effect of strongly non-linear modes, which tend to scatter particles out of collapsed regions. This "truncated Zel'dovich approximation" (hereafter TZA) was considerably refined and tested by Melott, Pellman and Shandarin (1993; hereafter MPS). They found that the optimal way to smooth the initial conditions is by convolution with a Gaussian filter whose radius is a specific, spectrum–dependent multiple of the scale of nonlinearity. TZA is a major improvement over ZA, and it as fast as one step in an N–body simulation. Any numerical implementation of ZA automatically truncates Fourier modes below the resolution limit (e.g. the Nyquist frequency in a grid code), but in TZA the truncation is handled in a controlled and optimized manner. In this paper, we will compare the adhesion approximation (hereafter AA) to N–body results and to ZA and TZA.

For a complete discussion of ZA, TZA, and AA, we refer the reader to the papers cited above. Here we limit ourselves to a simple physical description of AA, which can itself be regarded as an extension of ZA. With an appropriate choice of variables, ZA can be regarded as simple inertial motion, continuing the initial velocities of fluid elements (see e.g. Shandarin & Zeldovich, 1989). The approximation works much better than one might think based on this description, in large part because the potential has a larger coherence length than the density if the effective spectral index is $n \leq 1$. AA adds to the inertial motion a viscosity force $\nu \cdot \nabla^2 \mathbf{v}$, where $\mathbf{v}$ is the velocity and ν is the viscosity coefficient. This viscosity mimics some of the effects of nonlinear gravity, by eliminating the relative velocity of intersecting flows and causing fluid elements to "stick" when they fall into caustics. However, for finite ν this term is also nonzero in the voids, where the flow accelerates away from underdense perturbations, and in these regions it is likely to degrade the accuracy of the approximation.

The addition of the viscosity term to inertial motion yields Burgers' equation. If the initial velocity field is a potential flow (as expected in gravitational instability models), then Burgers' equation admits an exact integral expression for the velocity field at any later time. This integral can be evaluated by steepest-descent in the limit that the viscosity approaches (but does not equal) zero. In this approach (Gurbatov, Saichev and Shandarin 1985, 1989; Nusser and Dekel, 1990; Kofman, Pogosyan and Shandarin 1992; Kofman *et al.* 1992; Sahni, Sathyaprakash and Shandarin 1991), the pancakes are infinitely thin, and the flow is exactly that given by ZA outside of multistream regions. From a geometrical analysis of the velocity field, one can derive the skeleton of the structure (i.e. the location of sheets, filaments, and knots) at any time, but not a detailed distribution of matter inside collapsed regions.

In this paper we use the particle implementation of AA described by Weinberg and Gunn (1990). In this method, one evaluates the Burgers integral by Gaussian convolution, using a finite value of the viscosity parameter. The resulting code is closer in spirit to an N–body code; one integrates particle orbits, at each timestep using the velocity field implied by the solution to Burgers' equation.

II. SIMULATIONS

In our AA simulations, we used the smallest value of the viscosity that did not produce numerical overflows (see Weinberg and Gunn [1990] for further discussion). We checked the choice of timestep by comparing to similar runs with shorter timesteps. The adhesion simulations had initial conditions identical to one realization set of N–body simulations, described in Melott and Shandarin (1993). We used power law initial density fluctuation spectra, $P(k) \propto k^n$ for $n = -2, -1, 0, +1$. We chose for analysis in all of these the moment when rms fluctuations are just going nonlinear ($\delta\rho/\rho = 1$) at a wavelength of $L/8$, where L is the box size. At this output time, nonlinear structures are well resolved, but the scale of nonlinearity is small enough that the simulations' periodic boundary conditions do not cause problems. We also checked results at a later stage when the nonlinear wavelength was $L/4$. The N–body and adhesion simulations both used 128^3 particles on a 128^3 mesh.

Figures 1a, 2a, 3a, and 4a show slices one cell thick through the N–body simulations for the four initial power spectra. In these greyscale renderings, regions below the mean density are white, and regions above a density contrast of 10 are black. Figures 1b to 4b show corresponding slices from the adhesion simulations with the same initial conditions. Figures 1c to 4c show results from TZA, the most successful of the approximations previously tested in this series.

As noted elsewhere (e.g. Weinberg and Gunn [1990]), the adhesion simulations look more filamentary than the full N–body simulations. This is a reflection of the fact that their "superpancakes" (see Melott and Shandarin 1993) are less broken up into subcondensations. This difference in texture is more pronounced for larger values of n. Also, there seem to be some condensations in the adhesion model that have no counterparts in the N–body run, though this mismatch may be an artifact of plotting thin slices. Although the TZA figures have fewer objects than either of the others, their locations agree well with those of the primary condensations in the N–body run.

III. QUANTITATIVE COMPARISON

The most direct comparison we can make with N–body asks whether the adhesion simulations put mass in the same place. To address this question quantitatively, we study the cross–correlation of the adhesion models with the N–body models in the manner of CMS. We define the cross-correlation statistic S as

$$S = \frac{< \delta_1 \, \delta_2 >}{\sigma_1 \, \sigma_2} \, , \tag{1}$$

where δ_1 and δ_2 are the local density contrast in the N–body and adhesion simulations at the same spot, and σ_1 and σ_2 are the standard deviations of the two density fields. For identical density fields, $S = 1$. When the fields are defined at very high resolution, small errors in the precise positions of mass concentrations will destroy the correlation between them. We therefore compute S for a variety of Gaussian smoothings, which are applied in the same way to the two fields. The heavy lines in Figure 5 plot S against the value of σ in the smoothed N–body density field. The light lines plot S against σ for TZA. We see that:

(a) The match to N–body is worse for larger n, since initial conditions with more small scale power have more strongly nonlinear modes, which cannot be followed by the approximations.

(b) By comparison with CMS, we find that AA crosscorrelates about as well as ZA for $n = -2$, and better for all the other indices.

(c) In all cases, TZA performs better than AA on this test.

Figure 6 compares power spectra of the N–body simulations (heavy solid lines), the adhesion simulations (light solid lines), and TZA (light dashed lines). N–body and AA are shown at two epochs, when the nonlinear scale is $k_{nl} = L/8$ and $L/4$. TZA is shown only at $k_{nl} = L/8$. Small differences in the linear (small–k) part of the spectrum appear to be a numerical artifact of the N–body code, since both approximations agree better with linear perturbation theory in this regime. The error may be related to the very low fluctuation amplitude used in the initial conditions — one of us (DHW) has found similar behavior in a different code when starting from very small initial fluctuations. At its worst, it represents a 25% error in power after an expansion factor of about 5000.

The adhesion approximation underestimates large–k power, but it does a better job overall than any approximation tested so far. As we see from the dashed lines, TZA has a considerably larger error in the nonlinear part of the spectrum.

Distributions are characterized by both amplitudes and phases for their Fourier components. We tested for phase angle agreement by calculating $<\cos \theta>$, where θ is the difference in phase angle of the corresponding Fourier coefficients and the averaging is over spherical shells in wavenumber. Figure 7 plots $<\cos \theta >$ against k. As expected, the agreement declines steadily with increasing nonlinearity. The $n = +1$ model is substantially worse than the others, with gradual improvement through to $n = -2$ as n declines. MPS find the same trends for TZA. However, the phase errors for TZA are *smaller* than

those for AA. It is probably these smaller phase errors that account for TZA's higher cross–correlation with N–body.

Figure 8 plots the mass density distribution function: $N(\rho)$ is the number of cells with density in the range $\rho \rightarrow \rho + d\rho$. For this test, the density fields are defined by cloud-in-cell weighting of the 128^3 particle distributions onto a 64^3 mesh. Both AA and TZA underestimate the number of high–density pixels and overestimate the number of low– and moderate–density ones, but AA is much more successful here, as it is for the power spectrum.

IV. DISCUSSION

We summarize our conclusions and compare with previous work:

(a) The adhesion approximation is an substantial improvement over the original Zel'dovich (1970) approximation in all aspects of its performance (except, of course, computational speed).

(b) We measure AA's dynamical accuracy by cross–correlation with the N–body density fields. The agreement is quite good, but not as good as that found for the truncated Zel'dovich approximation by MPS.

(c) AA reproduces the N–body power spectrum and mass density distribution better than any other approximation that we have tested so far.

(d) AA makes greater errors than TZA in the phases of Fourier coefficients of the mass distribution.

(e) By combining the above results with our visual examination of the greyscale plots, we infer that AA is doing a reasonable job of making condensations but is putting them in somewhat incorrect positions.

(f) In most respects, AA performs better than the frozen–flow approximation – see Melott, Lucchin, Matarrese, and Moscardini (1993). However, AA is much more computer intensive than frozen–flow.

(g) Of the methods that we have studied to date, it appears that TZA is the best dynamical approximation, in the sense of moving mass to the right place. AA is the best statistical approximation, in that it comes closest to reproducing the statistical results of N–body simulations, at least for the $P(k)$ and $N(\rho)$ statistics that we have examined here.

It is not at all clear what are the intrinsic sources of errors in the adhesion particle method. In one test case, we found that doubling the value of the viscosity coefficient had almost no impact on the results, which suggests that finite viscosity of the amplitude that we are using here is not an important source of error. Gurbatov *et al.* (1985, 1989) applied the adhesion method in the limit of vanishing viscosity, using it to find the skeleton of structure, not the details of the mass distribution. That implementation of AA cannot be compared to N–body simulations in the same way as the particle–pushing implementation examined here, and it is not clear that it will make the same errors in locating collapsed structures. We think that further investigation of this question is warranted, but it is outside the scope of the present study. We should also note that we have compared AA

and TZA for one stage only, when $k_{nl} = 8k_f$. We found qualitatively similar results for $k_{nl} = 4k_f$, and we believe that our conclusions will hold for other stages as well.

If one wants a "poor man's N–body" method for evolving specified initial conditions, TZA has clear advantages over the particle implementation of AA: it is simpler, much faster, uses less memory, and produces more accurate results (in terms of cross–correlation). It has similar advantages over other approximations that we have tested. Babul *et al.* (1993) have used adhesion to generate initial conditions for simulations of the explosion scenario, and adhesion may provide a useful computational technique for other specific applications. However, the adhesion approximation will probably make its most important contributions as a tool for analytic calculations and as a source of physical insight into the formation of large–scale structure.

ACKNOWLEDGEMENTS

Our computations were performed at the National Center for Supercomputing Applications, Urbana, Illinois, USA. Research at the University of Kansas was supported by NASA grant NAGW–2923 and NSF grants AST–9021414 and NSF EPSCoR grant OSR–9255223. DHW is supported by the W. M. Keck Foundation and NSF grant PHY92-45317.

REFERENCES

Babul, A., Weinberg, D.H., Dekel, A. and Ostriker, J.P. 1993, ApJ, submitted
Coles, P., Melott, A.L and Shandarin, S.F. 1993, MNRAS 260, 765 (CMS)

Gurbatov, S.N., Saichev, A.I. and Shandarin, S.F. 1985, Sov.Phys.Dokl. 30, 921

Gurbatov, S.N., Saichev, A.I. and Shandarin, S.F. 1989, MNRAS 236, 385

Kofman, L., Pogosyan, D. and Shandarin, S.F. 1990, MNRAS, 242, 200

Kofman, L., Pogosyan, D., Shandarin, S.F. and Melott, A.L. 1992, ApJ 393, 437

Melott, A.L. and Shandarin, S.F. 1993, ApJ 410, 469

Melott, A.L., Pellman, T. and Shandarin, S.F. 1993, MNRAS, submitted (MPS)

Melott, A.L., Lucchin, F., Matarrese, S., and Moscardini, L. 1993, MNRAS, submitted

Nusser, A. and Dekel, A. 1990, ApJ 363, 14

Peebles, P.J.E. 1980, The Large–Scale Structure of the Universe, Princeton Univ. Press, Princeton, NJ

Sahni, V., Sathyaprakash, D. and Shandarin, S.F. 1993, in preparation

Shandarin, S., and Zeldovich, Ya.B. 1989, Rev.Mod.Phys. 61, 185

Weinberg, D.H. and Gunn, J.E. 1990, MNRAS 247, 260

Zel'dovich, Ya.B. 1970, Astr.Astrophys. 5, 84

FIGURE CAPTIONS

Figure 1: A greyscale plot of thin (L/128) slices through the simulation cubes for $n = +1$ initial conditions, at the stage when $k_{nl} = 8k_f$. (a) The N–body simulation. (b) The adhesion approximation (AA). (c) The optimum, Gaussian–truncated Zel'dovich approximation (TZA). All statistics below are calculated for this stage unless otherwise specified.

Figure 2: As in Figure 1, but for $n = 0$ initial conditions.

Figure 3: As in Figure 1, but for $n = -1$ initial conditions.

Figure 4: As in Figure 1, but for $n = -2$ initial conditions.

Figure 5: The cross–correlation S between the N–body density field and the density field of the approximate simulation (see equation [1]). Bold lines plot the cross–correlation for AA against the rms fluctuation of the N–body density field, after both fields are smoothed by convolution with identical Gaussian windows of various sizes. The initial power spectra are $n = +1$ (longdash/shortdash), $n = 0$ (shortdash), $n = -1$ (longdash), and $n = -2$ (dotdash). Lighter lines show the cross–correlation of TZA, for the same spectra.

Figure 6: Heavy solid lines show power spectra of the evolved N–body simulations at two stages ($k_{nl} = 8k_f$ and $4k_f$). Light solid lines show spectra of the adhesion simulations at the same epochs. Dashed lines show spectra from TZA (shown at only one stage, $k_{nl} = 8k_f$, to prevent confusion).

Figure 7: The average effective phase error in the adhesion simulations, quantified by $< \cos\ \theta >$ as described in the text. Different lines represent $n = +1$ (longdash/shortdash), $n = 0$ (shortdash), $n = -1$ (longdash), and $n = -2$ (dotdash).

Figure 8: The mass density distribution function in the N–body simulations (heavy solid lines), AA (light solid lines), and TZA (dashed lines). $N(\rho)$ is the number of cells with density (in units of the mean density) in the range $\rho \rightarrow \rho + d\rho$.

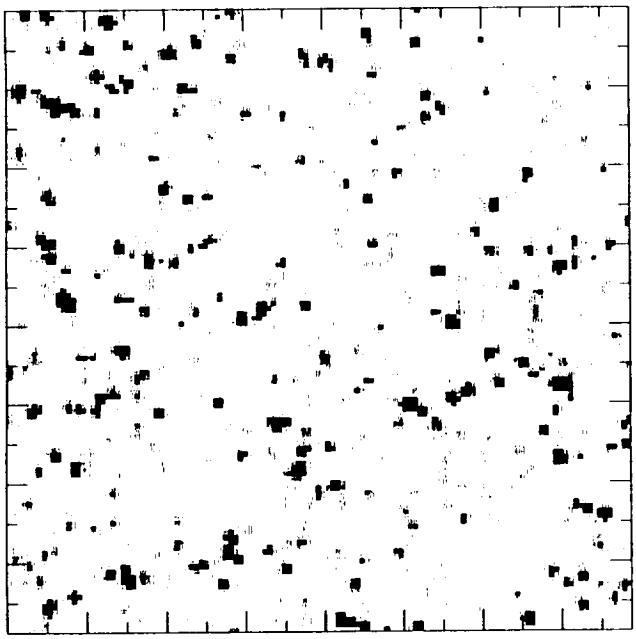

1a

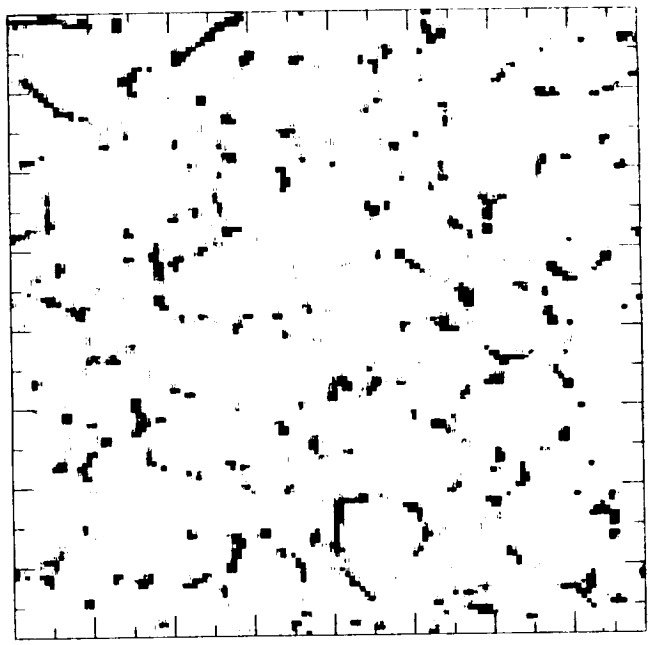

1b

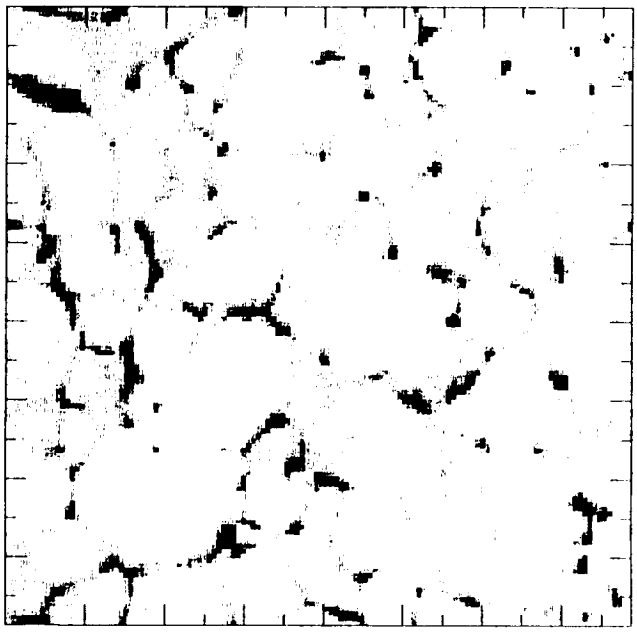

1c

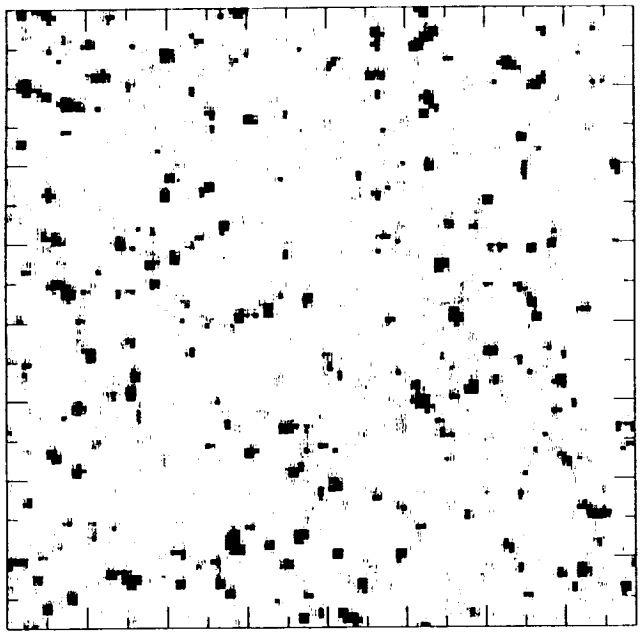

2a

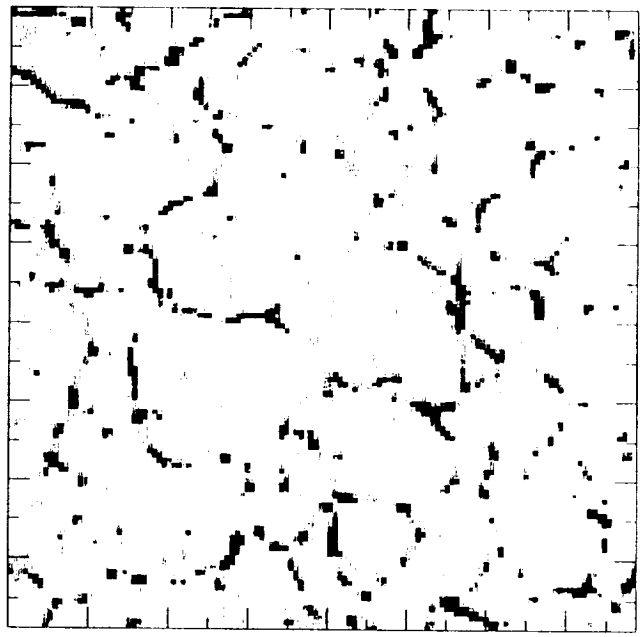

2b

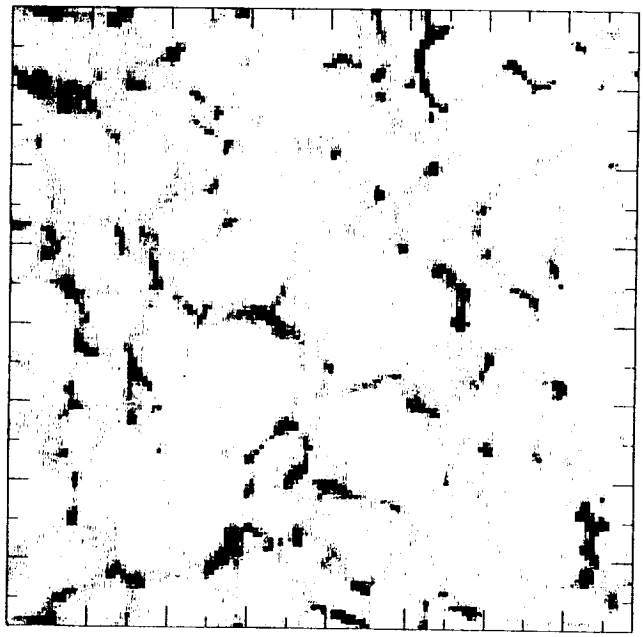

2c

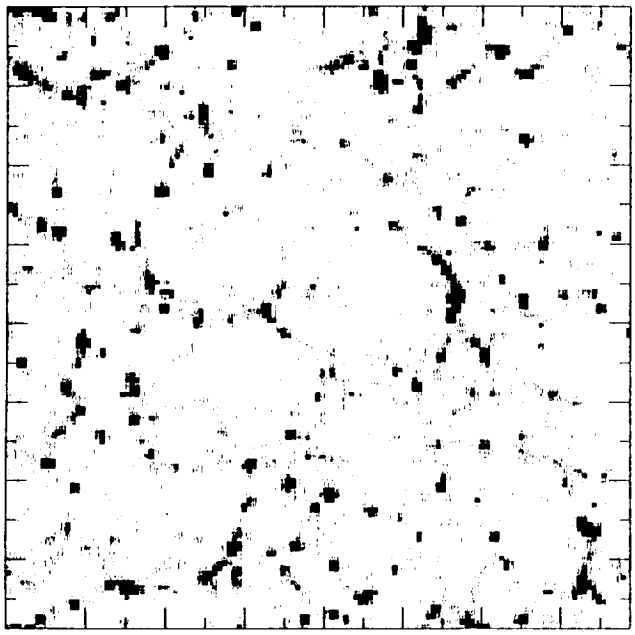

3a

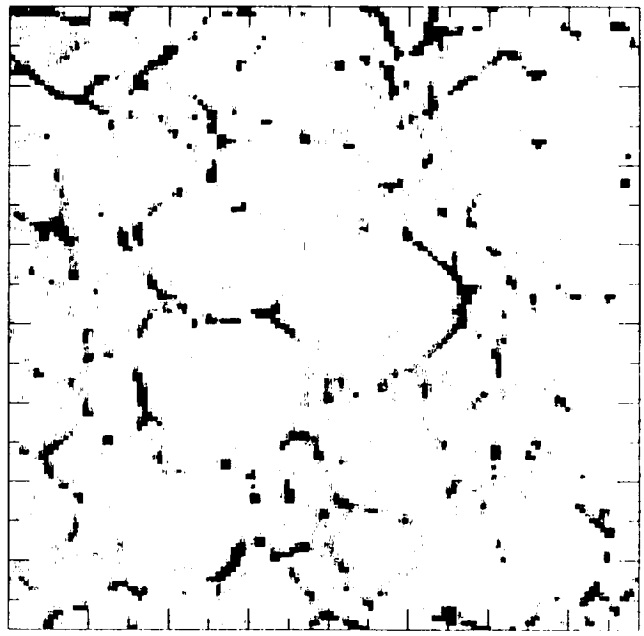

3b

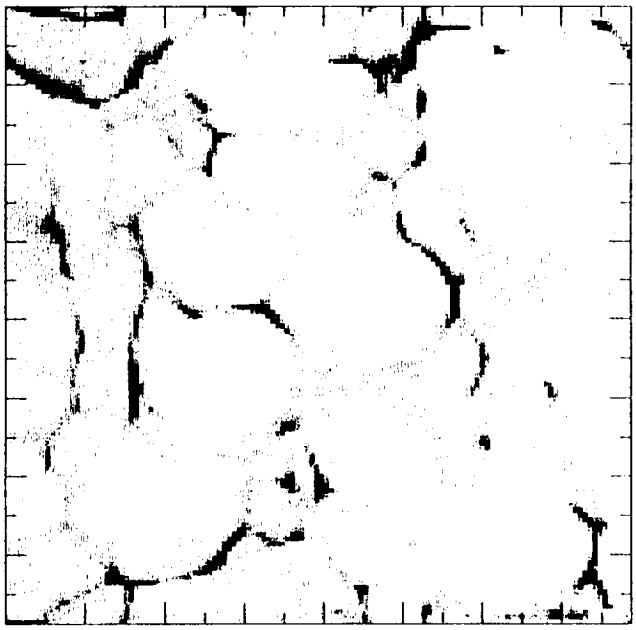

3c

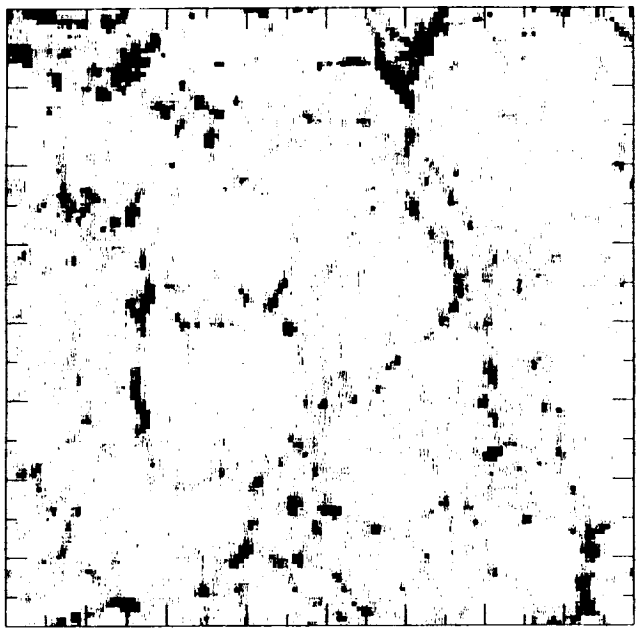

4a

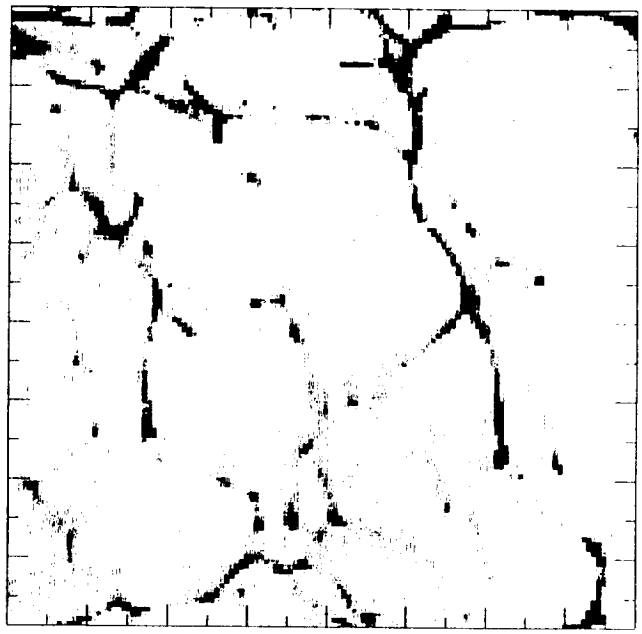

4b

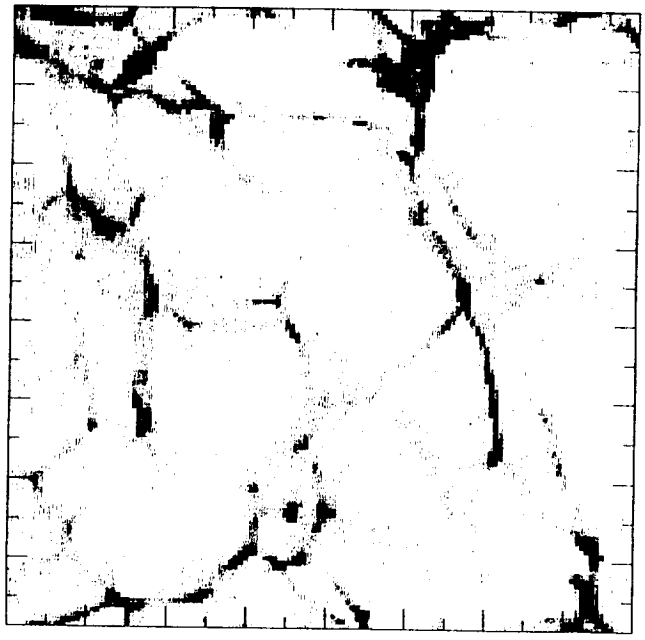

4c

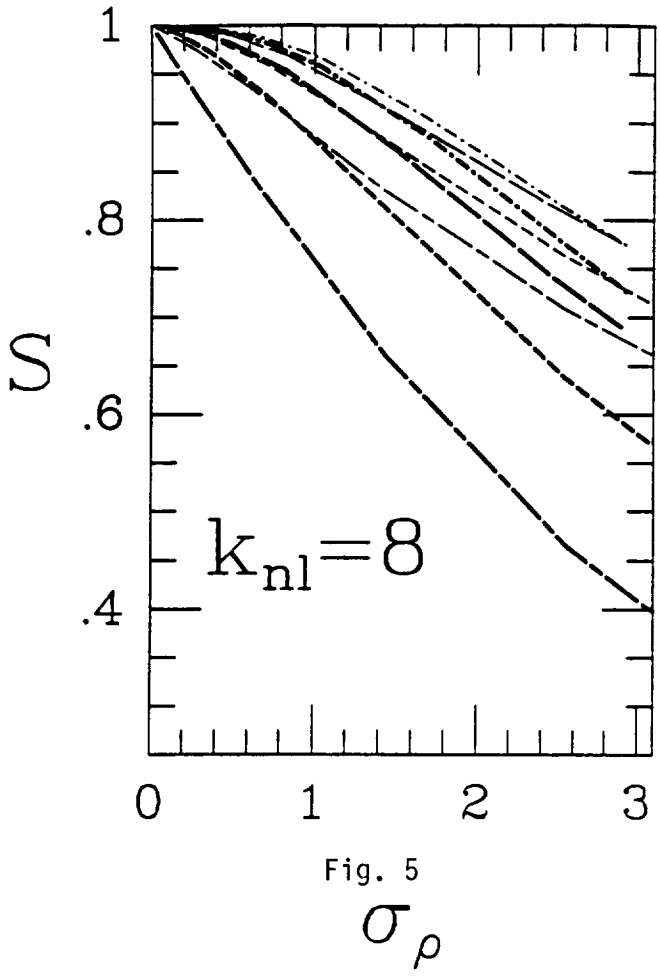

Fig. 5

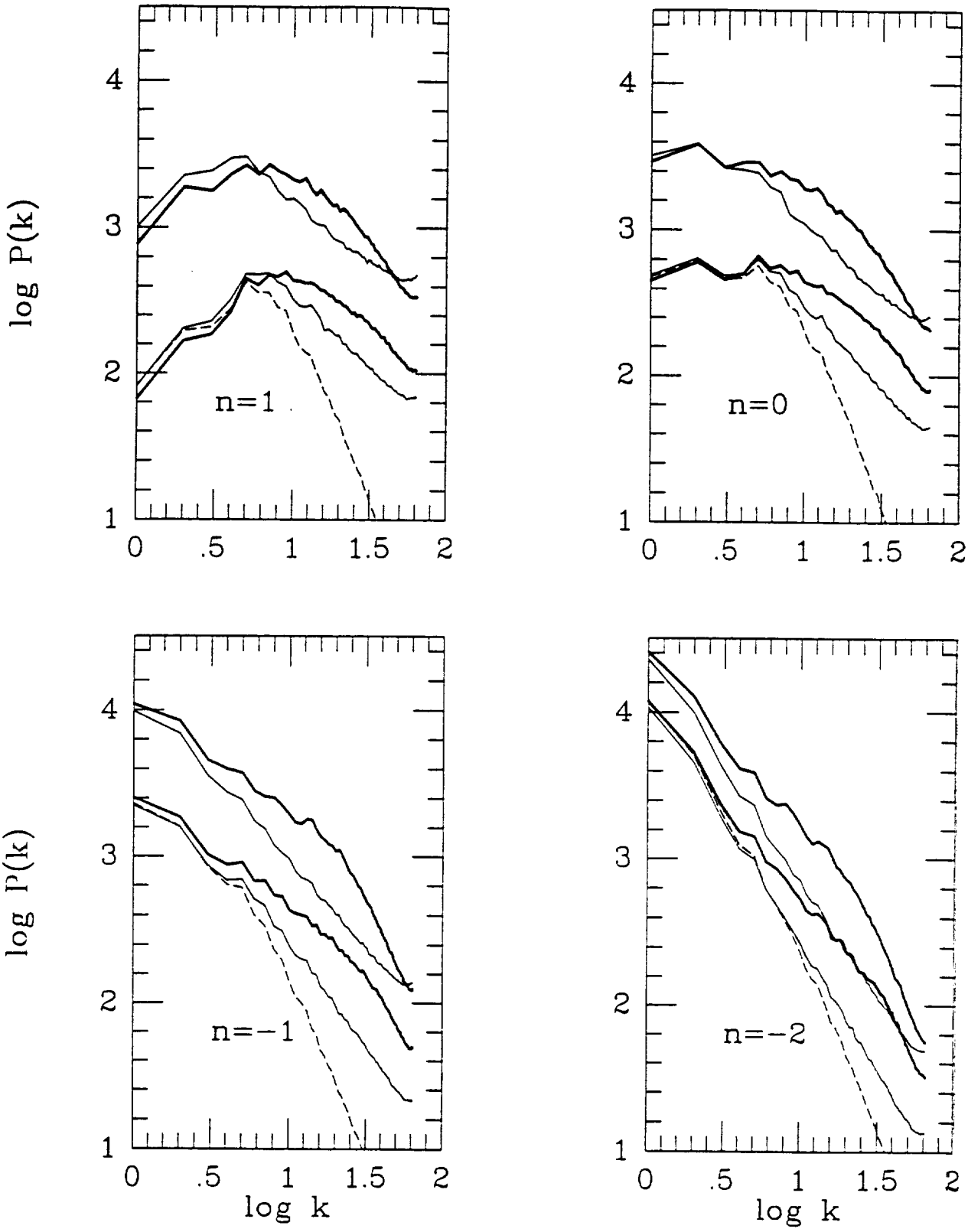

Fig. 6

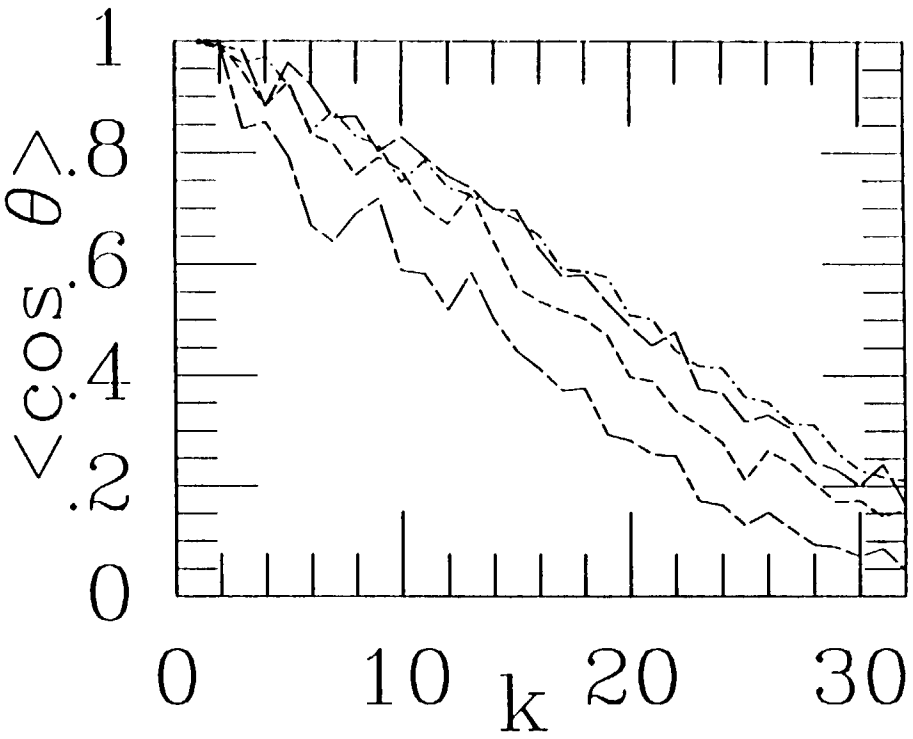

Figure 7

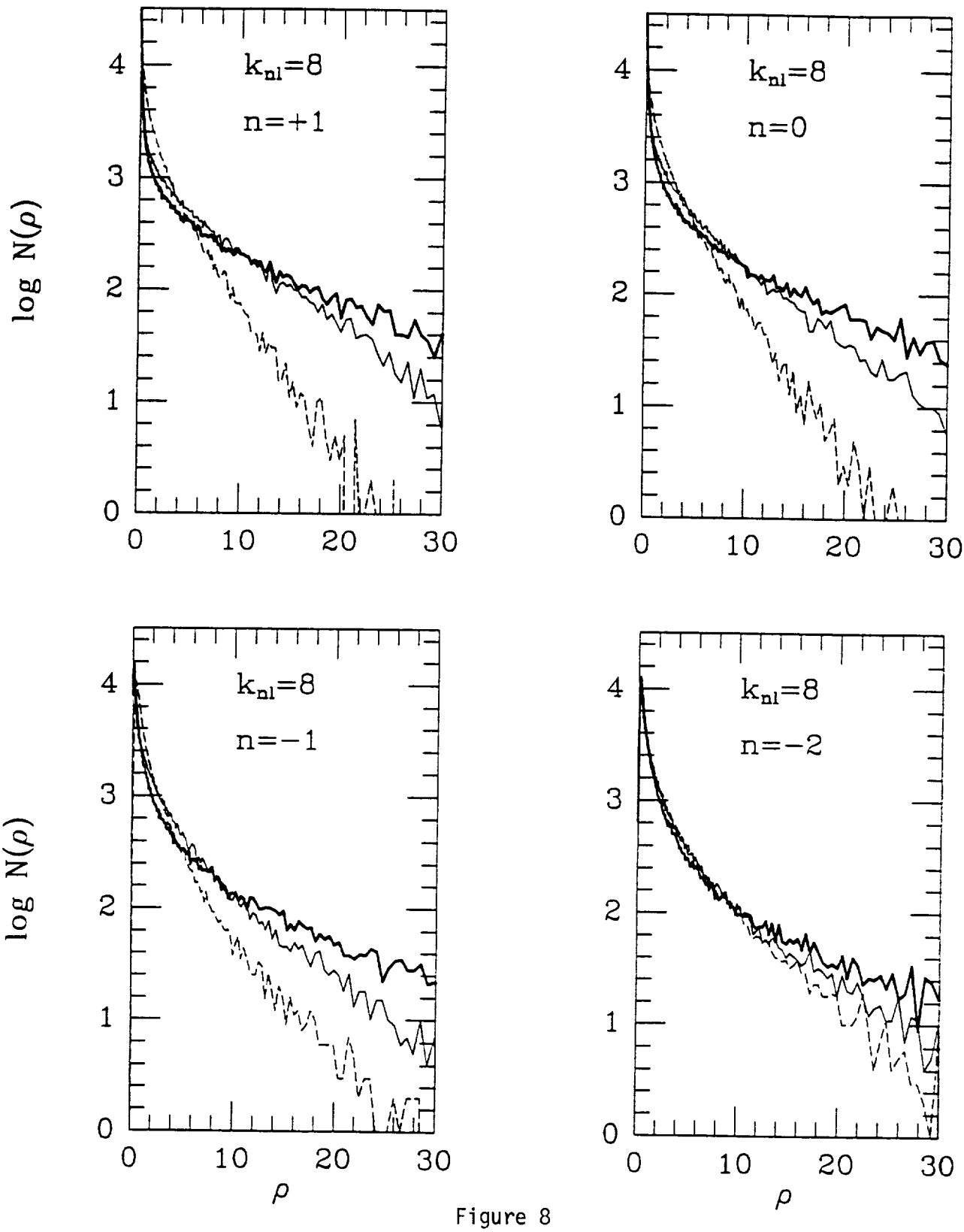

Figure 8